



## Iridium–silicide nanowires on Si(110) surface

Rasika N. Mohottige, Nuri Oncel \*

Department of Physics and Astrophysics, University of North Dakota, 101 Cornell Street, Witmer Hall, Grand Forks, ND 58202, United States



### ARTICLE INFO

#### Article history:

Received 23 March 2015

Accepted 14 July 2015

Available online 21 July 2015

#### Keywords:

STM

STS

Silicon 110

Nanowires

### ABSTRACT

We studied physical and electronic properties of iridium silicide nanowires grown on the Si(110) surface with the help of scanning tunneling microscopy and spectroscopy. The nanowires grow along the [001] direction with an average length of about 100 nm. They have a band gap of ~0.5 eV and their electronic properties show similarities with the iridium silicide ring clusters formed on Ir modified Si(111) surface.

© 2015 Elsevier B.V. All rights reserved.

Ir (Iridium)–silicides have the lowest (highest) Schottky barrier for holes (electrons) which can be used in various device applications on silicon. For example, among silicides, Pt (Platinum)–silicide/p-doped Silicon (Si) diodes are employed in large focal plane arrays for detection in the medium-wavelength infrared light (3–5  $\mu\text{m}$ ) [1]. The Schottky barrier height between Pt–silicide and p-doped Si(001) is about 0.23 eV corresponding to a cutoff wavelength of 5.4  $\mu\text{m}$  [2]. In order to extend the cutoff wavelength, it is necessary to choose interfaces with lower Schottky barrier height. The Schottky barrier height between Ir–silicide/p-doped silicon is approximately 0.17 eV corresponding to a cutoff wavelength of 7  $\mu\text{m}$  which makes Ir–silicide a promising material for infrared detector applications [3].

As continuous miniaturization challenges lithography techniques in electronics, self-assembly based processes become more attractive. One particularly important self-assembled component is metal–silicide nanowires. These nanowires can function as low-resistance interconnects, as fins in FinFET [4] devices and as nano-electrodes for attaching small electronic components within an integrated circuit. It has already been shown that a variety of metals form self-assembled silicide nanowires on the surface of flat and/or vicinal Si substrates [5–9]. Nanowires can be made up of various elements ranging from Bi [10] and rare-earth metals [11–13] to transition metals [14,15]. In comparison to Si(111) and Si(001) surfaces, Si(110) surface has received relatively less attention because the surface reconstruction is complicated and it is difficult to grow single large domains. However, higher hole mobility in devices fabricated on Si(110) surface and the possibility of employing self-assembled nanowires in various applications have recently increased number of studies on these systems [16–18]. Unlike 4-fold symmetric Si(001) surface, Si(110) surface is two-fold symmetric which can lead to formation of nanowires along the

same direction. Various studies have already reported the existence of metal–silicide nanowires on Si(110) [6,19,20,21–23]. In this letter, we report the formation of Ir–silicide nanowires.

The Si(110) samples used in the Scanning Tunneling Microscopy/Spectroscopy (STM/STS) experiments were cut from nominally flat 76.2 mm by 0.38 mm, single side-polished n-type (phosphorous doped,  $R = 1.0\text{--}10.0\ \Omega\text{-cm}$ ) wafers. The samples were mounted on molybdenum holders and contact of the samples to any other metal during preparation and experiment was carefully avoided. The STM/STS studies have been performed by using an ultra-high vacuum system (UHV) with a base pressure of  $2 \times 10^{-10}\ \text{mbar}$  equipped with an Omicron Variable Temperature STM. Before introducing Si(110) samples into the UHV chamber, samples were washed with isopropanol and dried under the flow of nitrogen gas. Si(110) samples were degassed extensively and after that flash-annealed at 1250 °C. Then the samples were annealed at various temperatures to obtain various reconstructions of pristine Si(110) and Ir–silicide nanowires (see details below). The sample temperature was measured with a pyrometer. The quality of the clean Si(110) samples was confirmed with STM prior to Ir deposition. Ir was deposited over the clean Si(110) surface from a current heated Ir wire (99.9%). All the STM experiments were performed at room temperature. I–V curves measured while measuring high resolution STM images of the surface. Then the measured I–V curves were averaged. The local density of states curves (LDOS) were calculated out of the I–V curves [24].

Fig. 1a and b show two STM images of pristine Si(110) surface before Ir deposition. It has been shown that the reconstruction of Si(110) surface depends strongly on the annealing temperature [25]. Annealing the sample at 600 °C leads to the formation of well-defined “16 × 2” domains however annealing at and above 800 °C, disordered phase forms (see Fig. 1a and b). So far, different structures have been proposed to explain Si(110)–“16 × 2” structure [26–28].

\* Corresponding author.

E-mail address: [nuri.oncel@und.edu](mailto:nuri.oncel@und.edu) (N. Oncel).

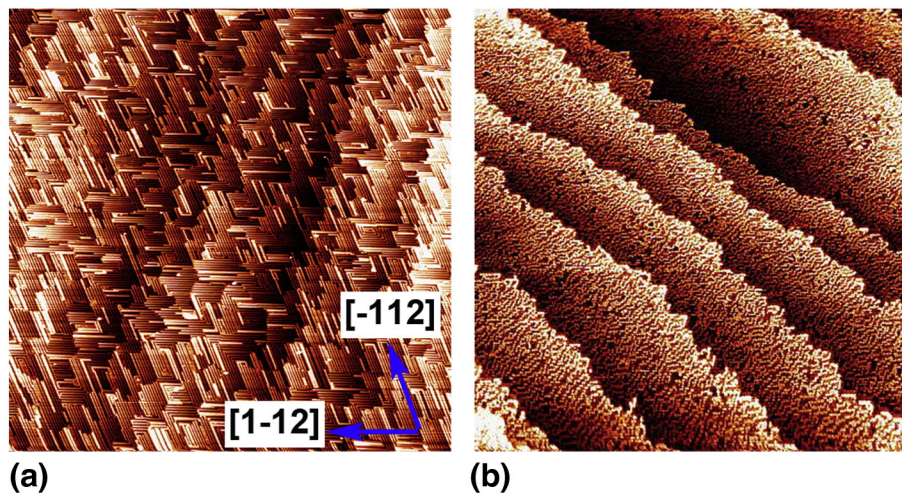


**Fig. 1.** a and b are the STM images of clean Si(110) annealed at 600 °C and 800 °C, respectively. The arrows indicate the high symmetry directions of the “16 × 2” domains. The sample bias and the tunneling current for the STM image in a (b) are –1.2 V (–1 V) and 0.2 nA (0.2 nA).

The ad-atom-tetramer-interstitial (ATI) is the most accepted of them [29,30]. According to this model, four ad-atoms of the top layer and one first layer atom come together and form a pentagon that surrounds an interstitial atom at its center.

After depositing 0.25 ML of Ir on the surface, the sample was annealed at 800 °C for two minutes while keeping the pressure below  $2 \times 10^{-10}$  mbar. Fig. 2a shows a large scale STM image of the surface where several nanowires are visible. The nanowires grow along the [001] direction. Fig. 2d shows a line scan graph measured on the

nanowire shown in Fig. 2b. The average height, length and width of nanowires are  $1.76 \text{ nm} \pm 0.32 \text{ nm}$ ,  $106.27 \text{ nm} \pm 21.76 \text{ nm}$  and  $14.63 \text{ nm} \pm 2.97 \text{ nm}$  respectively. The variances in length and width are correlated since the values closely follow the equation [31]:

$$\sigma_A^2 = \langle W \rangle^2 \sigma_L^2 + \langle L \rangle^2 \sigma_W^2 + 2\langle W \cdot L \rangle \sigma_{LW}$$

where  $\sigma_A$ ,  $\sigma_L$ ,  $\sigma_W$  are standard deviations of the area, the length and the width of the nanowires.  $\langle W \rangle$ ,  $\langle L \rangle$  stand for expectation value of the

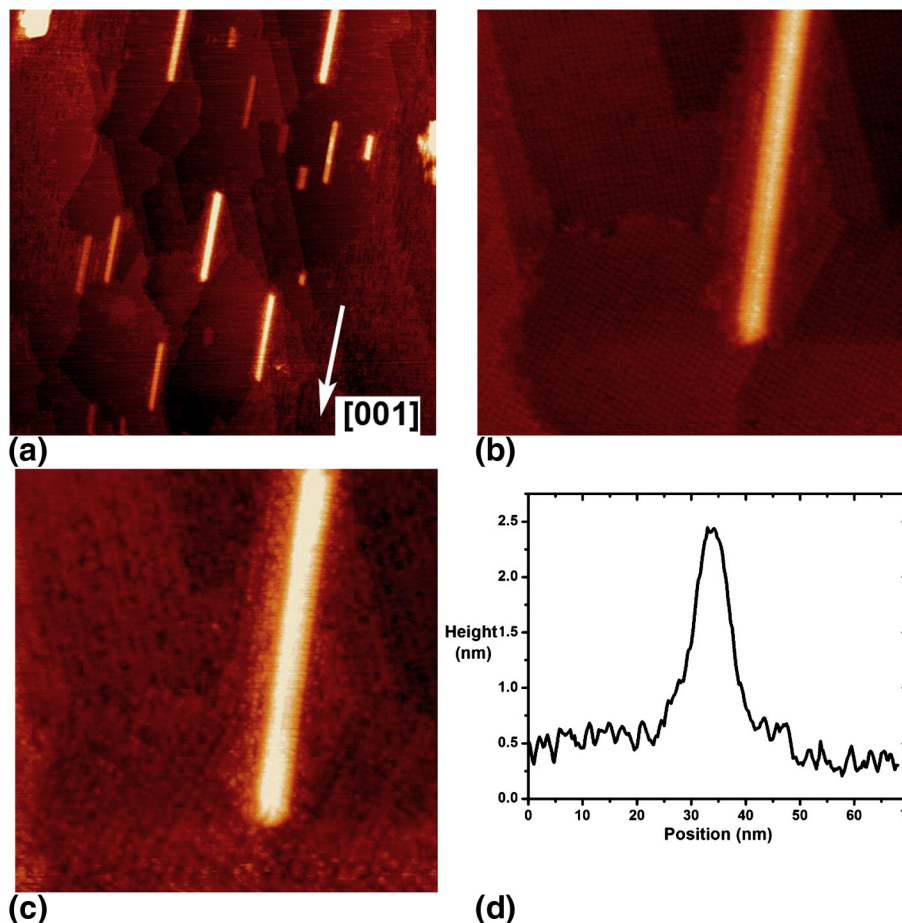


**Fig. 2.** (a) is a 400 nm × 400 nm and (b) is a 100 nm × 100 nm STM images of Ir modified Si(110) surface. Ir silicide nanowires grow along the [001] direction.

width and the length of the nanowires.  $\sigma_{LW}$  represents covariance of the width and the length of the nanowires. The strong correlation between the width and the length of a nanowire indicates that the length and the width must be physically coupled via strain, diffusion and etc.

High resolution STM images similar to Fig. 2b show that the terraces on which nanowires form have a superstructure that looks rather different than the pristine Si(110) surface. The superstructure has two equivalent domains that are rotated with respect to each other (see Fig. 3). Empty state image of the same region does not show any clear periodic structure (Fig. 2c). With the help of the matrix notation, the unit cell of the superstructure can be defined as (for domain A, see Fig. 3),

$$M_{\text{terrace}} = \begin{pmatrix} -4 & -1 \\ -2 & 3 \end{pmatrix}.$$

A careful analysis of STM images revealed that there are domain walls even within a single domain of the superstructure (see Fig. 3). These walls separate well-defined periodic regions, marked by the green rectangles. The domain walls are even thicker than the domains themselves indicating that the corrugation of the superstructure/substrate potential is significantly small compared to the lateral interactions between the constituents of this superstructure [32].

Kim et al. studied the electronic structure of Si(110)-“16 × 2” surface with angle resolved photoemission spectroscopy (ARPES) [33]. Their data show that there are four surface states located at −0.2 eV (S1), −0.4 eV (S2), −0.75 eV (S3) and −1.0 eV (S4). Later, with the help of STS measurements, the state at −0.2 eV was assigned to the pentagons and the rest of the states were attributed to the surface states at the step edges [34]. Fig. 4a shows the LDOS curve we measured. The LDOS curve reproduced most of the states below the Fermi level. One

important difference is that the LDOS curve has a just single peak located at −0.3 eV instead of two peaks at −0.2 eV and −0.4 eV as measured with ARPES. This can be due to the broadening of the STS peaks. The broadening corresponds to approximately 0.1 eV at room temperature [35]. LDOS data published by Setvín et al. also shows a single peak albeit their peak is located at 0.2 eV [36]. On the other hand, the LDOS graph has a shoulder at 0.3 eV and two well resolved peaks at 0.75 eV and 1.3 eV which are also attributed to pentagons on the surface [28].

Fig. 4b shows two LDOS curves measured on Ir–silicide nanowires (black) and the terrace (red) surrounding them. The nanowires and the terrace have band gap of about 0.5 V (see Fig. 4c) which is significantly wider than the band gap of “16 × 2” domains (~0.2 eV). Both LDOS curves have one well-resolved peak below the Fermi level. The peak coincides well with a well-known projected bulk band [33]. However, it can still have some surface contribution. Previously, we studied Ir ring clusters on Si(111) surface extensively [37,38]. Ab-initio density functional theory calculations performed on this surface revealed that below the Fermi level, there is a state associated with Ir atoms embedded in the ring clusters. The position of this state in the spectrum almost perfectly matches with the peaks observed on the Ir–silicide nanowires and the underlying terrace. Above the Fermi level, the LDOS curves in Fig. 4b look different. The terrace has a broader feature originating from conduction band. On the other hand, the nanowires have two well-resolved states located at 0.75 eV and 1.4 eV. The position of these peaks is comparable to the position of peaks measured on Ir ring clusters. On Ir ring clusters, we determined that these peaks belong to Ir atom and six Si adatoms that constitute the rings. Similarities on the electronic properties between the two surfaces suggest that the building blocks of these nanowires may resemble Ir-ring clusters.

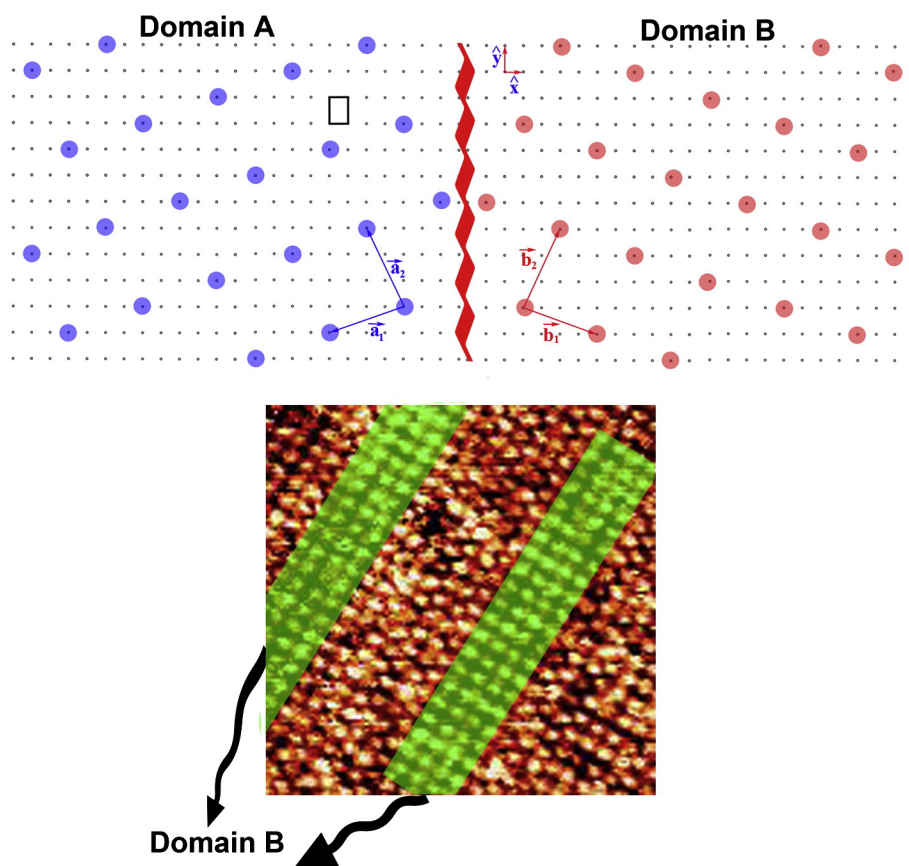


**Fig. 3.** Top: A schematic diagram of domain A (left) and domain B (right) of the superstructure is presented.  $\hat{x}$  and  $\hat{y}$  are basis vectors of Si(110) lattice pointing along [1–10] and [001] directions. Bottom: An STM image of the terrace showing the two B-type domains (green rectangles) separated by a domain wall. (For interpretation of the references to color in this figure legend, the reader is referred to the web version of this article.)

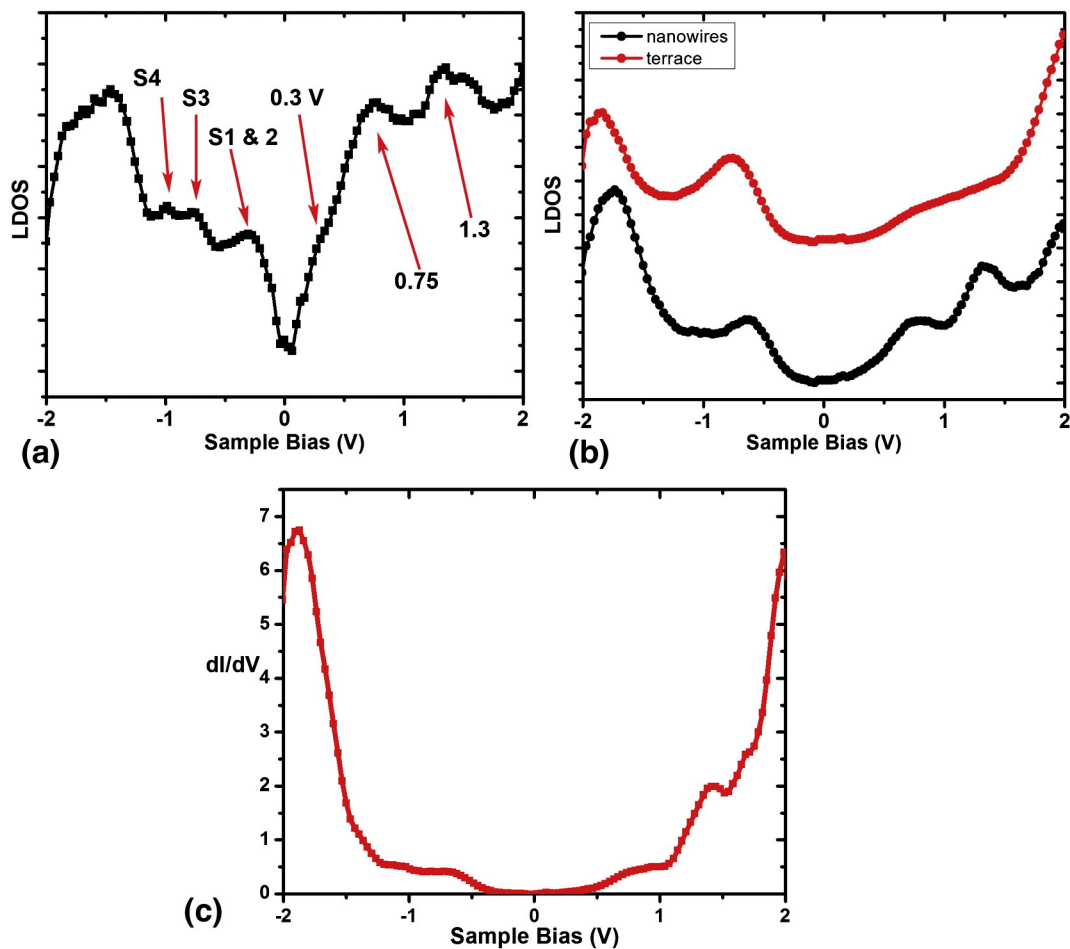


**Fig. 4.** (a) LDOS graph measured on pristine Si(110)-“16 × 2” surface. (b) LDOS graphs measured on Ir-silicide nanowires (black) and terrace surrounding the nanowires (red). (c)  $dI/dV$  graph measured on Ir-silicide nanowires that shows a gap of about 0.5 eV. (For interpretation of the references to color in this figure legend, the reader is referred to the web version of this article.)

In summary, we report the formation of Ir-silicide nanowires on Si(110) surface. The average length of a nanowire is about 100 nm. Statistical analysis of the size distribution reveals that the length and the width of the nanowires are correlated. This provides an opportunity to adjust the dimensions of these nanowires by changing growth parameters for the specific application. Ir-silicide nanowires are semiconductor with a band gap of about 0.5 eV. The position of the electronic states is similar to the Ir-ring cluster of Ir modified Si(111) surface. Although, we could not obtain an STM image that shows internal structure of the makings of the nanowires and the underlying superlattice, the similarities of the electronic properties between Ir-silicide nanowires and Ir-ring clusters suggest that the chemical composition of both surfaces may be similar.

#### Acknowledgment

This work was supported by NSF (# DMR-1306101).

#### References

- [1] W. Cabanski, R. Koch, H. Mainer, G. Paler, J. Wendler, J. Ziegler, K. Hofmann, K. Eberhardt, P. Daimel, U. Prechtl, K. Kapser, *Proc. SPIE* 2746 (1996).
- [2] A. Czernick, H. Palm, W. Cabanski, M. Schulz, U. Suckow, *Appl. Phys. A* 55 (1992) 180.
- [3] B.-Y. Tsauro, M.M. Weeks, P.W. Pellegrini, *IEEE Electron Device Lett.* 9 (1988) 100.
- [4] D. Hisamoto, W.-C. Lee, J. Kedzierski, H. Takeuchi, K. Asano, C. Kuo, E. Anderson, T.-J. King, F.J. Bokor, C. Hu, *IEEE Electron Device Lett.* 47 (2000) 2320.
- [5] Y.P. Zhang, L. Yang, Y.H. Lai, G.Q. Xu, X.S. Wang, *Appl. Phys. Lett.* 84 (2004) 401.
- [6] H. Okino, I. Matsuda, R. Hobaru, Y. Hosomura, S. Hasegawa, P.A. Bennett, *Appl. Phys. Lett.* 86 (2005) 233108.
- [7] A. Kida, H. Kajiyama, S. Heike, T. Hashizume, K. Koike, *Appl. Phys. Lett.* 75 (1999) 540.
- [8] R. Losio, K.N. Altmann, F.J. Himpsel, *Phys. Rev. Lett.* 85 (2000) 808.
- [9] J.R. Ahn, H.W. Yeom, H.S. Yoon, I.-W. Lyo, *Phys. Rev. Lett.* 91 (2003) 196403.
- [10] J.H.G. Owen, K. Miki, D.R. Bowler, *J. Mater. Sci.* 41 (2006) 4568.
- [11] Y. Chen, D.A.A. Ohlberg, G. Medeiros-Ribario, Y.A. Chang, R.S. Williams, *Appl. Phys. Lett.* 76 (2000) 4004.
- [12] Y. Chen, D.A.A. Ohlberg, R.S. Williams, *J. Appl. Phys.* 91 (2002) 3213.
- [13] J. Nogami, B.Z. Liu, M.V. Katkov, C. Ohbuchi, N.O. Birge, *Phys. Rev. B* 63 (2001) 233305.
- [14] O. Gurlu, O.A.O. Adam, H.J.W. Zandvliet, B. Poelsema, *Appl. Phys. Lett.* 83 (2003) 4610.
- [15] J. Wang, M. Li, E.I. Altman, *Phys. Rev. B* 70 (2004) 233312.
- [16] T. Sato, Y. Takeishi, H. Hara, Y. Okamoto, *Phys. Rev. B* 4 (1971) 1950.
- [17] A. Ciucivara, B.R. Sahu, S. Joshi, S.K. Banerjee, L. Kleinman, *Phys. Rev. B* 75 (2007) 113309.
- [18] Y. Liu, K. Ishii, T. Tsutsumi, M. Masahara, T. Sekigawa, K. Sakamoto, H. Takashima, H. Yamauchi, E. Suzuki, *IEEE Trans. On Nano.* 2 (2003) 198.
- [19] S. Liang, R. Islam, D.J. Smith, P.A. Bennett, J.R. O'Brien, B. Taylor, *Appl. Phys. Lett.* 88 (2006) 113111.
- [20] Z. He, D.J. Smith, P.A. Bennett, *Phys. Lett.* 93 (2004) 256102.
- [21] Z. He, M. Stevens, D.J. Smith, P.A. Bennett, *Appl. Phys. Lett.* 83 (2003) 5292.
- [22] S.M. Hus, H.H. Weitering, *Appl. Phys. Lett.* 103 (2013) 073101.
- [23] Z.-Q. Zou, G.-M. Shi, L.-M. Sun, X.-Y. Liu, *Appl. Phys. Lett.* 113 (2013) 024305.
- [24] J.A. Stroschio, R.M. Feenstra, A.P. Fein, *Phys. Rev. Lett.* 57 (1986) 2579.
- [25] Y. Yamada, A. Girard, H. Asaoka, *J. Phys. Conf. Ser.* 100 (2008) 072018.
- [26] T. An, M. Yoshimura, I. Ono, K. Ueda, *Phys. Rev. B* 61 (2000) 3006.
- [27] T. Ichikawa, *Surf. Sci.* 544 (2003) 58.
- [28] W.E. Packard, J.D. Dow, *Phys. Rev. B* 55 (1997) 15643.
- [29] A.A. Stekolnikov, J. Furthmuller, F. Bechstedt, *Phys. Rev. Lett.* 93 (2004) 136104.
- [30] A.A. Stekolnikov, J. Furthmuller, F. Bechstedt, *Phys. Rev. B* 70 (2004) 045305.
- [31] H. Ibach (Ed.) Springer, 2006.
- [32] Stuart L. Meyer (Ed.) Peer Management Consultants, Ltd, September 1992.

- [33] N.D. Kim, Y.K. Kim, C.-Y. Park, H.W. Yeom, H. Koh, E. Rotenberg, J.R. Ahn, *Phys. Rev. B* 75 (2007) 125309.
- [34] K. Sakamoto, M. Setvin, K. Matawari, P.E. Eriksson, K. Miki, R.I.G. Uhrberg, *Phys. Rev. B* 79 (2009) 045304.
- [35] C.J. Chen (Ed.) 2nd ed. Oxford Univ. Press, New York, 2008.
- [36] M. Setvín, V. Brázdová, D.R. Bowler, K. Tomatsu, K. Nakatsuji, F. Komor, K. Miki, *Phys. Rev. B* 84 (2011) 115317.
- [37] N. Oncel, D. Cakir, J.H. Dil, B. Slomski, G. Landolt, *J. Phys. Condens. Matter* 26 (2014) 285501.
- [38] D. Nicholls, N. Oncel, *J. Phys. Condens. Matter* 25 (2013) 445004.